DET NORSKE VIDENSKAPS-AKADEMI I OSLO

GEOFYSISKE PUBLIKASJONER
GEOPHYSICA NORVEGICA

Vol. XXVIII No. 5. January 1972

THOMAS A. MCCLIMANS

An Approximate Theory for the Structure of Strong Pycnoclines

OSLO 1972
UNIVERSITETSFORLAGET

GEOFYSISKE PUBLIKASJONER
GEOPHYSICA NORVEGICA
VOL. XXVIII NO. 5

AN APPROXIMATE THEORY FOR THE STRUCTURE OF STRONG PYCNOCLINES

By
Thomas A. McClimans

FREMLAGT I VIDENSKAPS-AKADEMIETS MØTE DEN 10. SEPTEMBER 1971 AV HØILAND

Summary. A simple model for the energetics of strong, turbulent pycnoclines is proposed for computing the structure below the depth of maximum gravitational stability. Turbulent exchange coefficients dependent upon both turbulent energy and stability show the strong coupling between turbulent energy flux and salt or heat flux. With the aid of some simplifying approximations and a minimum of empirical information the pertinent system of equations is integrated to give a theoretical structure in close agreement with that observed in fjord, ocean, and atmosphere.

Introduction. Typical examples of strong pycnoclines are fjord haloclines, ocean thermoclines, and atmospheric inversions. Previous theoretical investigations of the hydrographic structure of pycnoclines have not given a satisfactory explanation of the large density gradients observed in nature. The problem is usually treated with turbulent exchange coefficients chosen a priori as empirical functions.

It is well known that the exchange mechanism governing the structure of the pycnocline depends upon in situ turbulence and stability. This results in strong coupling between turbulent energy flux and salt (heat) flux. Munk and Anderson (1948) present a model in which the exchange coefficients are dependent upon shear stress and stability. Their analysis applies to the region above the depth of maximum stability for which the turbulence is predominantly dependent upon shear flow. The present treatment applies to the lower region of the pycnocline where the turbulent energy level is determined by diffusion from above. For the limiting case of strong pycnoclines, the depth of maximum stability approaches the depth of the homogeneous mixed layer as described by Tully (1958).

Model. Some elements of a model of a pycnocline are shown in Fig. 1 using fjord haloclines as examples. Here, river run-off forms a top layer which is homogenized by the action of wind, waves, and tidal currents. Through turbulent action this layer removes fluid from the lower layer, its salinity increasing seaward, and a region of

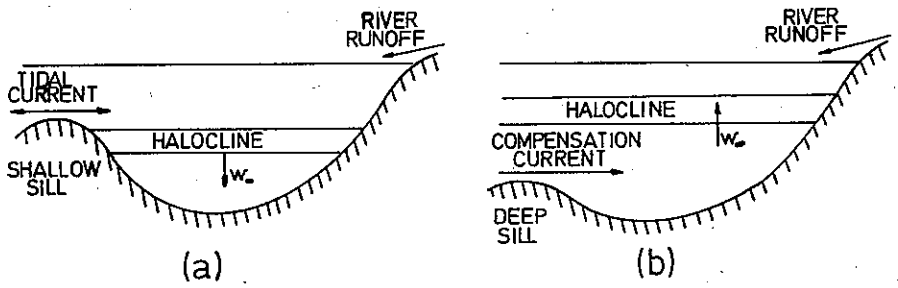

Figure 1. Schematic longitudinal sections of fjord haloclines: (a) erosion model with w_∞ = erosion velocity of the front, (b) steady-state model with w_∞ = vertical advection velocity of water through the halocline.

mixing with the lower fluid develops into a steady-state pycnocline. Variations of properties in the horizontal (x, y) direction can be considered negligibly small compared to variations in the vertical (z), taken positive downward.

A mixing process of this type, between two essentially homogeneous water masses, often appears as a straight line on the T—S diagram, implying local equality between exchange coefficients for salt and heat flux. For this case, either temperature or salinity can be used to describe the structure of the pycnocline, but the gravitational stability remains dependent on both variables.

Two variations of the model are shown schematically. The first model (Fig. 1 (a)) consists of a stagnant fluid layer above which erosion takes place. In this case the coordinates are fixed to the eroding front, assumed to have a constant rate of descent. This case is typical for shallow-silled fjords with a strong discontinuity layer and for air masses contained by a strong inversion. The second model (Fig. 1 (b)) consists of a stationary front in which a vertical advection of the fluid maintains the position of the pycnocline. A necessary element of this model is a compensation current. This case is typical of strong haloclines in deep-silled fjords and of oceanic thermoclines.

Turbulence is assumed to be generated at or above the depth of greatest stability $z=z_1$ and diffused downwards. The source of turbulence is pictured as a result of the transfer of turbulence from the surface layer, the breaking of large amplitude internal waves, Kelvin-Helmholtz instabilities induced by internal waves, and Reynolds stresses resulting from the large velocity gradients at the top of the layer. Turbulence generated at the bottom is not taken into account.

The steady-state velocity shear within the region below z_1 is assumed negligible. Anomalous shear layers of the type observed by Woods (1968) are regarded as a part of the stochastic process at very low frequencies.

The turbulent energy spectrum at each point in the region is assumed to have the following character: the energy input occurs predominantly through pressure fluctuations in the inertial sub-range corresponding to internal gravity waves. The energy flux in wave-number space is considered to be essentially absorbed by the increase of gravitational potential energy within the sub-buoyancy regime (Phillips 1966, p. 233) with a negligible flux to the dissipation regime. This model is best fulfilled at z_1 and

could serve as a measure for classifying "strong pycnoclines" since the usual Richardson number criterion does not apply in the absence of velocity shear. For the sake of analysis it will be assumed that dissipation is negligible throughout the entire lower region. Thus, the net energy supplied to the region is assumed to be consumed by the increase of potential energy of the fluid.

Theory. In the absence of friction, the mechanical energy equation is

$$\boldsymbol{v} \cdot \left[\frac{D\boldsymbol{v}}{dt} + \frac{1}{\rho} \nabla p - \boldsymbol{g} \right] = 0 \tag{1}$$

where $\boldsymbol{v}$ is velocity, ρ density, p pressure and $\boldsymbol{g}$ the acceleration of gravity. For an incompressible fluid, the conservation of mass implies $D\rho/dt = 0$ and with $\boldsymbol{v} \cdot \boldsymbol{g} \equiv g\boldsymbol{v} \cdot \nabla z$, (1) becomes

$$\frac{D\phi}{dt} = \frac{\partial p}{\partial t} \tag{2}$$

where

$$\phi \equiv \rho \frac{\boldsymbol{v} \cdot \boldsymbol{v}}{2} + p - \rho g z \tag{3}$$

is the total energy density. With the elimination of hydrostatic equilibrium in (2), ϕ contains the total kinetic energy density and turbulent energy densities p' and $g\rho' z'$, in which z' is the vertical displacement of a particle from its hydrostatic equilibrium within a density gradient.

The velocity field is $\boldsymbol{v} = \overline{\boldsymbol{v}} + \boldsymbol{v}'$ where the overhead bar represents a stochastic mean, with $\overline{\boldsymbol{v}} = -w_\infty \nabla z$, and the prime denotes turbulent fluctuations. Here, w_∞, the velocity of the eroding front (z_1) of the pycnocline, is small compared to the vertical turbulent fluctuation w'. Thus ϕ is essentially the total turbulent energy density.
With a turbulent field stationary relative to z_1, the stochastic average of (2) reduces to the divergence of the total turbulent energy flux

$$\overline{\frac{D\phi}{dt}} = 0 = \nabla \cdot \overline{\boldsymbol{v}\phi} \tag{4}$$

With a horizontal divergence negligible compared to the vertical divergence, (4) becomes

$$\frac{\partial}{\partial z}(\overline{w\phi}) = 0 \tag{5}$$

in which the stochastic mean represents integration over sufficient time and horizontal extent to suppress stochastic fluctuations.

Both w and ϕ have stochastic means and fluctuations. Thus

$$\frac{\partial}{\partial z}[-w_\infty \bar{\phi}(z) + \overline{w'\phi'}] = 0 \tag{6}$$

for which triple correlations representing energy fluxes of various sorts are implicit.

A corresponding expression for salt transport is

$$\frac{\partial}{\partial z}[-w_\infty \bar{s}(z) + \overline{w's'}] = 0 \tag{7}$$

where $\bar{s}(z)$ represents the mean salinity and s' the turbulent fluctuation. A similar expression is obtained for heat transfer.

Analysis. To solve (6) and (7) for the structure of a halocline $\bar{s}\ (z)$, a relation relating w' to ϕ in terms of the stability, and analytic expressions for the correlations $\overline{w'\phi'}$ and $\overline{w's'}$ are needed. This is accomplished by a series of approximations involving a mixing-length concept.

The turbulent gravitational potential energy density of a particle within a region of constant gravitational stability $d\bar{\rho}/dz$ is

$$g\rho' z' = gz'^2 \frac{d\bar{\rho}}{dz} \tag{8}$$

The distance a particle lies from its equilibrium position is

$$z' = \int_0^t w'(t',z)dt' \tag{9}$$

in which $t'=0$ is taken at the moment the particle crosses its equilibrium position. The stochastic mean of the turbulent gravitational potential energy is thus

$$\overline{g\rho' z'} = g\tau^2 \overline{w'^2} \frac{d\bar{\rho}}{dz} \tag{10}$$

in which τ is a weighted time period characteristic of the turbulent energy spectrum.

In addition to the assumption that particle displacements occur within an essentially constant density gradient it will be further assumed that τ varies little throughout the pycnocline compared to variations in $\overline{w'^2}$, and is to be considered constant.

Since the gravitational potential energy depends only upon the vertical component of turbulent velocity, an assumption of constant partition of ϕ among the three orthogonal coordinates yields

$$\bar{\phi} = \rho \overline{w'^2} \left(K_1 + K_2 \frac{d\bar{\rho}}{dz} \right) \tag{11}$$

in which K_1 is a partition constant for neutral stability and $K_2 \equiv g\tau^2 K_1/\rho$ is a weighting factor which accounts for the linear effect gravitational stability has upon the turbulent field. For the development which follows, ρ in (11) will be replaced by the density at large depth, ρ_∞, without serious error, so that K_2 is independent of z.

For a fjord halocline in which the salinity gradient is the dominant cause of stability, the density to a good approximation is

$$\rho = \rho_f + K_3 s \tag{12}$$

in which ρ_f is the density for fresh water, $s=\bar{s}+s'$ is the salinity (‰) and $K_3\cong 0.0008$ gr. cm^{-3} (‰)$^{-1}$. A corresponding expression for the case when the temperature gradient is a measure of stability gives $K_3\cong -0.0002$ gr. cm^{-3} (°C)$^{-1}$, although this varies somewhat with temperature and salinity.

The correlation $\overline{w'\phi'}$ in (6) represents a selfdiffusion process. For this, a mixing length model similar to (10) can be used (see Appendix). With ϕ' a linear function of z', the stochastic mean becomes

$$\overline{w'\phi'}=K_4\overline{w'^2}\frac{d\bar{\phi}(z)}{dz} \tag{13}$$

where K_4, a period characteristic of the turbulent spectrum, contains the average local correlation between w' and ϕ'. As with τ, K_4 can be considered essentially constant with depth. The term $K_4\overline{w'^2}$ acts as an exchange coefficient dependent upon in situ turbulence and stability.

A similar development for the transfer of salt gives

$$\overline{w's'}=K_5\overline{w'^2}\frac{d\bar{s}(z)}{dz} \tag{14}$$

in which K_5 contains the average correlation between w' and s', which, unlike K_4, is negative.

As a result of turbulent "diffusion", the pycnocline extends to infinite depth. At some large depth the exchange coefficients approach limiting values as stability and energy consumption vanish. A lower bound for the analysis is chosen at an arbitrary depth $z=z_2$ for which $d\overline{w'^2}/dz\cong 0$ and

$$\overline{w'^2}(z_2)=K_6{w_\infty}^2 \tag{15}$$

where K_6 is a constant for each pycnocline. The condition $d\overline{w'^2}/dz=0$ corresponds to an exponential density profile, which is in good agreement with hydrographic observations far beneath the depth of maximum stability.

Structure of a strong pycnocline. With (14), the integral of (7) from $z=\infty$ is

$$-w_\infty\bar{s}(z)+K_5\overline{w'^2}\frac{d\bar{s}(z)}{dz}=-s_\infty w_\infty \tag{16}$$

where s_∞ is an asymptotic value of $s(z)$ at large depth. The transformations

$$\xi\equiv\frac{s_\infty-\bar{s}(z)}{s_\infty-s_1}\equiv\frac{s_\infty-\bar{s}(z)}{\Delta s}\equiv\frac{\rho_\infty-\bar{\rho}(z)}{\Delta\rho} \tag{17}$$

and

$$\zeta\equiv\frac{z_2-z}{-w_\infty K_5K_6}\equiv\frac{z_2-z}{L} \tag{18}$$

combine with (16) to give

$$\xi(\zeta){w_\infty}^2=\frac{\overline{w'^2}}{K_6}\dot{\xi}(\zeta) \tag{19}$$

in which $\dot{\xi}(\zeta) \equiv d\xi(\zeta)/d\zeta$. Here $s_1 \equiv \overline{s}(z_1)$ is the average salinity at the depth of maximum stability and L is a characteristic length giving the proper scaling. For $z=z_2$, $\zeta=0$ and from (15), $\xi(0)=\dot{\xi}(0)$. The same equation is obtained for heat flux.

With (17) and (19), the turbulent energy density (11) is

$$\overline{\phi} = K_1 K_6 w_\infty{}^2 \rho_\infty \frac{\xi}{\dot{\xi}}(1+K\dot{\xi}) \tag{20}$$

where $K \equiv g\varepsilon(\tau^2/L)$, with $\varepsilon \equiv \Delta\rho/\rho_\infty$, is a ratio between the reduced gravity and an acceleration associated with the turbulent field.

With (13) and (17)—(20), (6) becomes, after some algebra

$$\frac{d}{d\zeta}\left[\frac{\xi}{\dot{\xi}}\frac{d}{d\zeta}\left(\frac{\xi}{\dot{\xi}}\right)\right] = K(R-1)\dot{\xi} + R\frac{d}{d\zeta}\left(\frac{\xi}{\dot{\xi}}\right) \tag{21}$$

where $R \equiv K_5/K_4$. Integration of (21) twice from $\zeta=0$ gives

$$\left(\frac{\xi}{\dot{\xi}}\right)^2 = A_1 \int_0^\zeta \xi d\zeta' + A_2 \int_0^\zeta \left(\frac{\xi}{\dot{\xi}}\right) d\zeta' + A_3\zeta + 1.0 \tag{22}$$

where $A_1 \equiv 2K(R-1)$, $A_2 \equiv 2R$ and $A_3 \equiv -\xi_0 A_1 - A_2$, with $\xi_0 \equiv \xi(0)$. Here, a term $d(\xi/\dot{\xi})/d\zeta$ evaluated at $\zeta=0$ has been dropped by virtue of the expected asymptotic behavior of $\xi(\zeta)$ for small ζ.

With the identity $\dot{\xi}/\xi = d(\ln\xi)/d\zeta$, (22) is integrated to the exponential form

$$\xi(\zeta) = \xi_0 \exp\left[\int_0^\zeta \left(A_1 \int_0^{\zeta'} \xi d\zeta'' + A_2 \int_0^{\zeta'} \left(\frac{\xi}{\dot{\xi}}\right) d\zeta'' + A_3\zeta' + 1.0\right)^{-\frac{1}{2}} d\zeta'\right] \tag{23}$$

The positive root is used because ξ has its least value for $\zeta=0$.

Since the constant 1.0 dominates the integral in (23) for small ζ, the profile is an approximate exponential function at that depth. This justifies a posteriori the omission of the term $[d(\xi/\dot{\xi})/d\zeta]_{\zeta=0}$ and allows for a direct numerical integration. The solution $\xi(\zeta+\Delta\zeta)$ is calculated from integrals based upon the solution at ζ with $\Delta\zeta \to 0$.

The profile $\xi(\zeta)$, representing the structure of the pycnocline, is dependent upon R, K and a reference value ξ_0. At the depth of maximum stability $\zeta_m \equiv (z_2-z_1)/L$, $\xi(\zeta_m)=1.0$.

Evaluation of parameters. Numerical integration of (23) for some finite reference value ξ_0 requires the evaluation of K and R, which are functions of the turbulence. The dominance of pressure fields in the transport of energy implies $R \ll 1$, as for momentum transport.

The parameter K is evaluated from a minimum of empirical information for the limiting case of strong stability. As ε increases, $R \to 0$ (Ellison and Turner (1959)) and $w_\infty \to 0$ (Turner 1968)) giving $\overline{\phi}(\infty) \to \overline{\phi}(z_1)$, in the absence of molecular effects.

With $\xi(0)/\dot{\xi}(0)=\xi(\zeta_m)=1.0$, the solution of (21) for $R=0$ gives the constraint $K\leq 1.0$. The requirement $\overline{\phi}(\infty)/\overline{\phi}(z_1)\leq 1.0$ gives the constraint

$$K\geq 1.0-\frac{1}{\dot{\xi}(\zeta_m)} \tag{24}$$

since ξ_0 is vanishingly small. Observations show that $\dot{\xi}(\zeta_m)\gg 1$ for strong pycnoclines (e.g., Defant (1961), p. 119), so the approximation $K\cong 1.0$ will be used for the limiting case.

The strong pycnocline is a self-regulating system of in situ turbulence and stability, for which the maximum stability acts as a control point. For that part of the turbulent spectrum for which vertical fluctuations are governed by gravitational stability, the quotient of the scaled vertical turbulent accelerations L/τ^2 and $g\varepsilon$ remains essentially constant as ε varies. Consequently, $K\cong 1.0$ is expected to apply to a large range of stabilities.

Solutions of (23) for the limiting values $R=0$ and $R=-1.0$ and the limiting value of $K=1.0$, representing strong pycnoclines, are shown in Fig. 2. A weak dependence upon R is apparent. The ordinate is relative, depending upon the location of the reference value ξ_0. Integration from $\xi_0=0.001$ gives essentially the same results as integration from smaller values. The exponential structure representing molecular diffusion is also shown in Fig. 2.

Comparison with observations. To compare the theory with observations, it is necessary to compute the parameters giving the proper scaling. The parameters s_∞, ε, L and ξ_0 are calculated directly from the hydrography with at least three observations in the exponential region $z\cong z_2$ and one observation at the depth of maximum stability $z=z_1$. Clearly $\overline{s}(z_1)$ is difficult to determine without detailed measurements unless it coincides with the bottom of a homogeneous mixed layer, as Tully (1958) suggests[1].

Numerical schemes involving three equidistant observations s_{N-1}, s_N and s_{N+1} in the vicinity of z_2 do not give satisfactory results. The computational accuracy improves as $(s_N-s_{N-1})/(s_{N+1}-s_N)\to 1.0$ in which case the accuracy of the measurements becomes critical. This is remedied by passing an asymptotically smooth curve through the three observations and using gradients.

The relation

$$s_\infty=\overline{s}(z)+L\frac{d\overline{s}(z)}{dz} \tag{25}$$

is satisfied at two depths near $z\cong z_2$, and

$$\xi_0=\frac{L}{\Delta s}\frac{d\overline{s}(z)}{dz}\bigg|_{z=z_2} \tag{26}$$

is evaluated from $\overline{s}(z_1)$.

[1] The depth of maximum stability is left unspecified. It is to be computed by the theory on the basis of the observations in the lower region.

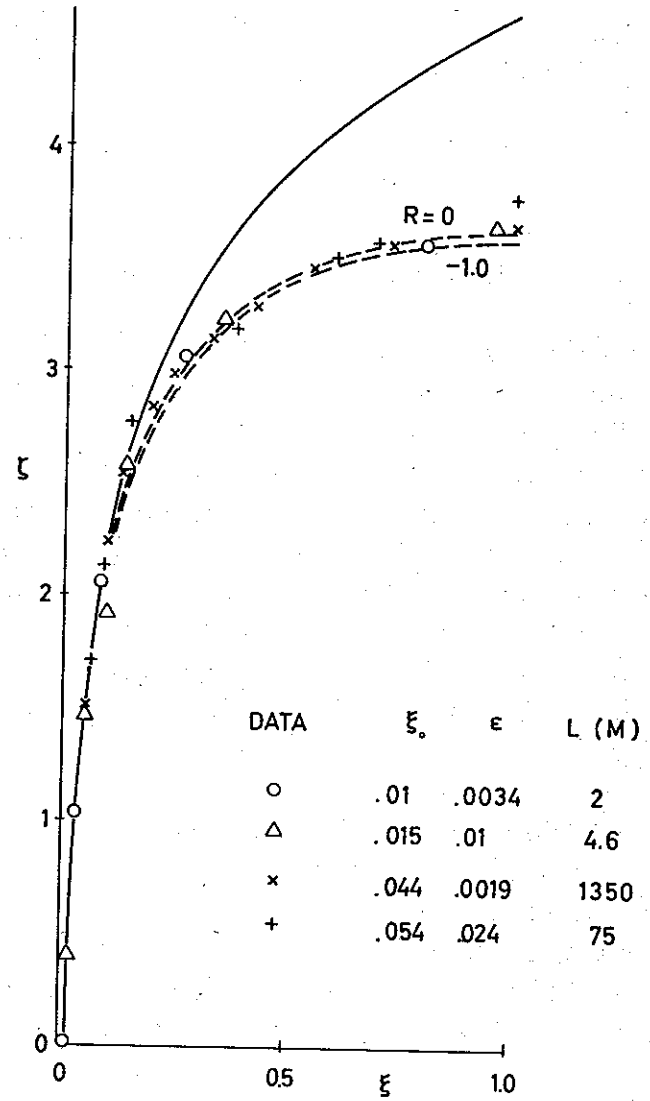

Figure 2. Hydrographic structure of strong pycnoclines below the depth of maximum gravitational stability. Theory: ——— molecular diffusion, — — — turbulent exchange. Data: ⊙ Borgenfjorden, salinity; △ Hardangerfjord, salinity; × Indian Ocean, temperature; + Blindern, adiabatic air temperature. Parametric values noted.

The data presented in Fig. 2 fulfill the requirements of the theory to a satisfactory degree. In Borgenfjorden (Strømgren et al. (1969)) the bottom water is stagnant and the rate of erosion is constant for a period of many weeks. The air layer at Blindern (Sivertsen (1969)) is stationary for several days.

In Hardangerfjord[1] there is established a compensation current at 20—30 m depth below which lie the remains of an earlier halocline. The temperature data for the Indian Ocean (Defant (1961, p. 118)) are mean values taken over a long-term stochastic process. A region of almost neutral stability at 500 m depth appears as a small perturbation at $\zeta = 3.4$.

[1] Unpublished data, courtesy International Biological Project P. M. Section, Norway.

The data imply that $K=1.0$ applies to a wide range of conditions and that there is no essential difference between salinity and temperature structure. Clearly, the turbulent structure is fundamentally different from the molecular diffusion structure. The approximate theory divides the structure of the pycnocline, below the depth of maximum stability, rather accurately into a region of exponential decay and a region of strong stability, described earlier by Tully (1958).

Discontinuity layer. If the region of large stability is interpreted as a "discontinuity layer' or "inversion layer", its thickness is approximately L. This layer extends from the depth of maximum stability to the depth at which 85% of the total density difference is observed, and serves as a measure for comparative studies. Within this region vertical exchange is greatly reduced.

Exchange coefficients. A vertical exchange coefficient for salt flux is, from (14), $A_z \equiv K_5 \overline{w'^2}$. This coefficient is largest in the homogeneous mixed layer above the pycnocline, is least at the depth of maximum stability, and increases with depth to an asymptotic value $A_z(\infty) = K_5 K_6 w_\infty{}^2$, as shown by Wyrtki (1961). From the definition of L (18), the exchange coefficient at large depth is

$$A_z(\infty) = L w_\infty \tag{27}$$

which, for a shallow-silled fjord can be calculated from the hydrography taken at two separate times. For the ocean, Wyrtki calculates w_∞ from the heat budget.

Since $\overline{\phi}(z)$ varies little throughout a strong pycnocline, the distribution of exchange coefficient with depth, derived from (11), (14), (27), and the definitions of K_2 and K, is approximately

$$A_z(z) \cong L w_\infty \left(1 + \frac{L}{\Delta\rho}\frac{d\overline{\rho}(z)}{dz}\right)^{-1} \tag{28}$$

A similar expression for the horizontal exchange coefficient $A_x \equiv K_5 \overline{u'^2}$, with $\overline{u'^2} = \overline{\phi}/K_1$ expressing equipartition of energy between the z and x components gives

$$\frac{A_x(z_1)}{A_z(z_1)} = 1 + \frac{L}{\Delta\rho}\frac{d\overline{\rho}}{dz}\bigg|_{z=z_1} \tag{29}$$

at the depth of maximum stability. Due to advection currents in the homogeneous mixed layer, observed values of A_x/A_z are often orders of magnitude larger than (29).

Discussion. A striking feature of strong pycnoclines is the "discontinuity layer" within which gravitational stability plays a significant role in damping out the vertical turbulent exchange process. An approximate transport theory with exchange coefficients linearly dependent upon both in situ turbulent energy level and stability describes satisfactorily the structure of strong pycnoclines below the depth of maximum stability.

The term "strong pycnocline" has been qualified twice: in the formulation of the energy flux, dissipation was rendered negligible, and in the empirical evaluation of K, $\xi(\zeta_m) \gg 1.0$ was used. It is important that the total turbulent energy density is essentially constant throughout the region below the depth of maximum stability. The success of the present theory in predicting the structure is due to the fact that the primary role of stability is not the production of potential energy, but rather the reduction of the vertical transport properties of the fluid. The importance of energy flux reduces as $R \to 0$.

The characteristic length L is a measure of the turbulent environment. It has a direct relation to the vertical exchange process and can be used in comparative analyses.

Assuming the turbulent pycnocline to be a uniquely defined phenomenon in the ξ, ζ coordinates, systematic deviations from the computed structure can be interpreted in terms of physical processes different from those taken into account by the theory. This was already seen in the temperature structure for the Indian Ocean. It is not clear whether the perturbation has a hydrodynamic or hydrographic cause; however, the hydrography is a composite of two thermoclines separated by a 100 m layer of neutral stability which appears to have a passive role in the transfer of turbulent energy. As another example, observations from Sognefjorden (Skofteland (1970)) matched, after trial and error, a fully developed structure of a strong halocline corresponding to a larger-than-observed salinity in the homogeneous mixed layer. With the aid of a T—S diagram, this was diagnosed as a rapidly decreasing salinity in the upper layer, presumably a result of spring flood. The exponential tail of the pycnocline is an integrated result of past events which can be used to estimate changes in external conditions from observations at one point in time. This can, in principle, extend the interpretive value of hydrography.

Acknowledgement. This work emerged from a series of lectures I gave in 1969 on fjord circulation. I wish to thank the participating students and my colleagues A. Green, E. Høiland, E. Palm, O. H. Sælen and Ph. Thompson for stimulating discussions on various aspects of the problem.

Appendix. Criterion for turbulent self-diffusion.

Consider the mixing length model of Prandtl, but with the lump of fluid moving inviscidly in quiescent fluid surroundings. The induced velocity field contains an energy which is proportional to the kinetic energy of the fluid lump in motion. This field, producing local pressure fluctuations, moves with the lump so that the actual energy transport associated with the motion contains a particle convection and a field convection, expressed as $\frac{\partial \phi}{\partial t} = -\nabla \cdot v\phi - \nabla \cdot vc\phi$ with c a constant. This expresses the conservation of ϕ within the reaches of the induced fields.

Due to the similarity of field convection and particle convection, the usual mixing length concept can be applied. It requires only that the effective reach of the fields

is contained within a linear $\overline{\phi}$ gradient. A comparison of Prandtl's momentum transfer theory with Taylor's vorticity transfer theory, in which pressure transfer is implicit (Schlichting (1955)), gives $c = 1.0$ for momentum transfer.

The criterion for application of mixing length theory to energy transport is $\frac{\partial p}{\partial t} = -cv \cdot \nabla\phi$. Recent results of Nee and Kovasznay (1969) support the concept of self-diffusion of turbulent energy according to (13).

REFERENCES

Defant, Albert, 1961: Physical oceanography, Vol. 1. The Macmillan Co., New York. 729 pp.

Ellison, T. H. and Turner, J. S., 1959: Mixing of dense fluid in a turbulent pipe flow. Part 2. Dependence of transfer coefficients on local stability. *J. fluid Mech.*, **8**: 529—544.

Munk, W. H. and Anderson, E. R., 1948: Notes on the theory of the thermocline. *J. mar. Res*, **7**: 276—295.

Nee, V. W. and Kovasznay, L. S. G., 1969: Simple phenomenological theory of turbulent shear flows. *Phys. Fluids*, **12**: 473—484.

Phillips, O. M., 1966: The dymanics of the upper ocean. Cambridge University Press, London, 259 pp.

Schlichting, H., 1955: Boundary Layer Theory. Pergamon Press, New York. 535 pp.

Sivertsen, Bjarne, 1969: En meteorologisk undersøkelse av luftforurensning. Cand.real. dissertation, University of Oslo, Blindern, 54 pp.

Skofteland, Egil, 1970: Hydrografiske undersøkelser i indre del av Sognefjorden. Rapport no. 3/70. Vassdragsdirektoratet, Hydrologisk Avdeling, Oslo. 65 pp.

Strømgren, Tor, et al. (8 authors), 1969: Borgenfjordundersøkelsene: Preliminærrapport. Det Kgl. Norske Videnskabers Selskab-Museet, Trondheim. 65 pp.

Tully, J. P., 1958: On structure, entrainment and transport in estuarine embayments. *J. mar. Res.*, **17**: 523—535.

Turner, J. S., 1958: The influence of molecular diffusivity on turbulent entrainment across a density interface. *J. fluid Mech.*, **33**: 639—656.

Woods, J. D., 1968: Wave-induced shear instability in the summer thermocline. *J. fluid Mech.*, **32**: 791—800.

Wyrtki, Klaus, 1961: The thermohaline circulation in relation to the general circulation in the oceans. *Deep-Sea res.*, **8**: 39—64.

Papers published in *Geofysiske Publikasjoner* may be obtained from: Universitetsforlaget, Blindern, Oslo 3, Norway.

Vol. XXIII.

No. 1. Bernt Mæhlum: The sporadic E auroral zone. 1962.
» 2. Bernt Mæhlum: Small scale structure and drift in the sporadic E layer as observed in the auroral zone. 1962.
» 3. L. Harang and K. Malmjord: Determination of drift movements of the ionosphere at high latitudes from radio star scintillations. 1962.
» 4. Eyvind Riis: The stability of Couette-flow in non-stratified and stratified viscous fluids. 1962.
» 5. E. Frogner: Temperature changes on a large scale in the arctic winter stratosphere and their probable effects on the tropospheric circulation. 1962.
» 6. Odd H. Sælen: Studies in the Norwegian Atlantic Current. Part II: Investigations during the years 1954—59 in an area west of Stad. 1963.

Vol. XXIV.

In memory of Vilhelm Bjerknes on the 100th anniversary of his birth. 1962.

Vol. XXV.

No. 1. Kaare Pedersen: On the quantitative precipitation forecasting with a quasi-geostrophic model. 1963.
» 2. Peter Thrane: Perturbations in a baroclinic model atmosphere. 1963.
» 3. Eigil Hesstvedt: On the water vapor content in the high atmosphere. 1964.
» 4. Torbjørn Ellingsen: On periodic motions of an ideal fluid with an elastic boundary. 1964.
» 5. Jonas Ekman Fjeldstad: Internal waves of tidal origin. 1964.
» 6. A. Eftestøl and A. Omholt: Studies on the excitation of N_2 and N_2^+ bands in aurora. 1965.

Vol. XXVI.

No. 1. Eigil Hesstvedt: Some characteristics of the oxygen-hydrogen atmosphere. 1965.
» 2. William Blumen: A random model of momentum flux by mountain waves. 1965.
» 3. K. M. Storetvedt: Remanent magnetization of some dolerite intrusions in the Egersund Area, Southern Norway. 1966.
» 4. Martin Mork: The generation of surface waves by wind and their propagation from a storm area. 1966.
» 5. Jack Nordø: The vertical structure of the atmosphere. 1965.
» 6. Alv Egeland and Anders Omholt: Carl Størmer's height measurements of aurora. 1966.
» 7. Gunnvald Bøyum: The energy exchange between sea and atmosphere at ocean weather stations M, I and A. 1966.
» 8. Torbjørn Ellingsen and Enok Palm: The energy transfer from submarine seismic waves to the ocean. 1966.
» 9. Torkild Carstens: Experiments with supercooling and ice formation in flowing water. 1966.
» 10. Jørgen Holmboe: On the instability of stratified shear flow. 1966.
» 11. Lawrence H. Larsen: Flow over obstacles of finite amplitude. 1966.

Vol. XXVII.

No. 1. Arne Grammeltvedt: On the nonlinear computational instability of the equations of one-dimensional flow. 1967.
» 2. Jørgen Holmboe: Instability of three-layer models in the atmosphere. 1968.
» 3. Einar Høiland and Eyvind Riis: On the stability of shear flow of a stratified fluid. 1968.
» 4. Eigil Hesstvedt: On the effect of vertical eddy transport on atmospheric composition in the mesosphere and lower thermosphere. 1968.
» 5. Eigil Hesstvedt: On the photochemistry of ozone in the ozone layer. 1968.
» 6. Arnt Eliassen: On meso-scale mountain waves on the rotating earth. 1968.
» 7. Kaare Pedersen and Knut Erik Grønskei: A method of initialization for dynamical weather forecasting, and a balanced model. 1969.

A.s John Griegs Boktrykkeri